
# Type 2 diabetes is related to neurochemical alterations in the default mode network: An exploratory cross-sectional Magnetic Resonance Spectroscopy study

Kia Puustinen , Jitske Vandersmissen , Tin Gojevic , Georg Oeltzschner , Helge J. Zöllner , Kenneth Verboven , Dominique Hansen , Ilse Dewachter , Melina Hehl , Koen Cuypers

PII: S1053-8119(26)00264-8
DOI: https://doi.org/10.1016/j.neuroimage.2026.121949
Reference: YNIMG 121949

To appear in: *NeuroImage*

Received date: 9 February 2026
Revised date: 8 April 2026
Accepted date: 21 April 2026

Please cite this article as: Kia Puustinen , Jitske Vandersmissen , Tin Gojevic , Georg Oeltzschner , Helge J. Zöllner , Kenneth Verboven , Dominique Hansen , Ilse Dewachter , Melina Hehl , Koen Cuypers , Type 2 diabetes is related to neurochemical alterations in the default mode network: An exploratory cross-sectional Magnetic Resonance Spectroscopy study, *NeuroImage* (2026), doi: https://doi.org/10.1016/j.neuroimage.2026.121949

**Highlights**

- T2DM group showed reduced tNAA and tCho (PFC), tCr (PCC), and GSH (hippocampus)
- Various brain metabolite levels may be correlated to blood glucose control
- Considering glucose control as a continuum might offer more sensitivity
- HERCULES $^{1}$H-MRS allowed more metabolites to be quantified simultaneously
- Findings suggest regional alterations in brain energy metabolism in T2DM

# Type 2 diabetes is related to neurochemical alterations in the default mode network: An exploratory cross-sectional Magnetic Resonance Spectroscopy study

Kia Puustinen [1, 2, 3], Jitske Vandersmissen [1, 5, 6], Tin Gojevic [5], Georg Oeltzschner [4], Helge J. Zöllner [4], Kenneth Verboven [5, 6], Dominique Hansen [5, 6, 7], Ilse Dewachter [6], Melina Hehl [8, 1, 2, 3], Koen Cuypers [1, 2, 3]

1. Neuroplasticity and Movement Control Research Group, REVAL Rehabilitation Research Centre, Hasselt University, Diepenbeek, Belgium
2. Leuven Brain Institute (LBI), KU Leuven, Leuven, Belgium
3. Movement Control and Neuroplasticity Research Group, Department of Movement Sciences, Group Biomedical Sciences, KU Leuven, Heverlee, Belgium
4. Russell H. Morgan Department of Radiology and Radiological Science, The Johns Hopkins University School of Medicine, Baltimore, MD, United States
5. Rehabilitation and Exercise Physiology in Cardiometabolic Diseases Research Group, REVAL Rehabilitation Research Centre, Hasselt University, Diepenbeek, Belgium
6. BIOMED Biomedical Research Institute, Faculty of Medicine and Life Sciences, Hasselt University, Diepenbeek, Belgium
7. Heart Centre Hasselt, Jessa Hospital, Hasselt, Belgium
8. Translational MRI, Department of Imaging & Pathology, KU Leuven, Belgium

**Corresponding author:** Koen Cuypers, Ph.D.
Faculty of Rehabilitation Science, Hasselt University
Wetenschapspark 7, 3590 Diepenbeek, Belgium
E-mail: koen.cuypers@uhasselt.be



## Abstract

**Background.** Type 2 diabetes mellitus (T2DM) is a chronic metabolic disorder linked to an increased risk for neurodegeneration and cognitive impairment. The current study set out to

explore a wide range of indirect markers of neuronal function via proton magnetic resonance spectroscopy ($^{1}$H-MRS) to help elucidate the link between altered glucose metabolism and neurodegeneration.

**Method.** Adults with T2DM (*n* = 20) and age- and sex-matched control subjects (*n* = 20) underwent fasted blood sampling, Montreal Cognitive Assessment, and $^{1}$H-MRS using a novel sequence HERCULES, allowing the reliable quantification of small and overlapping signals, adding to the number of quantifiable metabolites.

**Results.** Significant neurometabolic differences were observed in three brain regions. Namely, N-acetylaspartate (tNAA) and total choline (tCho) in the medial prefrontal cortex, total creatine (tCr) in the posterior cingulate cortex, and glutathione (GSH) in the hippocampus were lower in the T2D group than the control group. Glycated hemoglobin was inversely correlated with prefrontal tCho, tNAA, and tCr levels, as well as posterior cingulate tCr. In contrast, glycated hemoglobin was positively correlated with prefrontal concentrations of glutamate, along with left sensorimotor cortex glutamate, glutamine, myo-inositol, and lactate.

**Conclusion.** The region-specific metabolic deficits in tNAA, tCho, tCr, and GSH observed in the default mode network add to our understanding of diabetic encephalopathy. These exploratory findings might support a deficit model of brain energy metabolism and raise clinically relevant research questions about the neuro-energetic underpinnings of cognitive impairment in T2DM.

***Keywords:*** Type 2 diabetes, $^{1}$H-MRS, default mode network, cognitive impairment, brain metabolism

## 1. Introduction

Type 2 diabetes mellitus (T2DM) affects nearly 10% of the world population, and its prevalence is projected to rise in the coming decades (Sun et al., 2022) . Its large burden of disease can be attributed both directly to poor blood glucose control, as well as its consequences on various insulin sensitive tissues and organs (Heni, 2024). For example, in the brain, chronic hyperglycemia and hyperinsulinemia disrupt energy metabolism, driving maladaptive changes in mitochondrial function (Moreira et al., 2007; Raza et al., 2015), neuroinflammation (Maciejczyk et al., 2019), and cellular senescence in neurons (Chow et al., 2019). In fact, T2DM can result in widespread neurodegeneration (Yao et al., 2021). Disrupted insulin sensitivity has also been identified as central to Alzheimer's disease (AD) (Alves et al., 2021), and similar to AD, neurodegeneration in T2DM has been observed to disproportionately affect the brain's default mode network—a collection of brain regions active while a person is not actively engaging in a goal-oriented task (Kullmann et al., 2016; Raichle, 2015; Yao et al., 2021).

In addition to functional and structural brain changes, some researchers have captured the effects of hyperglycemia on neurometabolism by using proton magnetic resonance spectroscopy ($^{1}$H-MRS). The most consistent findings in T2DM, as compared to non-diabetic control subjects, include diminished total N-acetylaspartate (tNAA), and elevated myo-inositol (mI) and choline-containing compounds (tCho) (Duarte, 2016; Wu et al., 2017). Brain concentrations of tNAA are known to positively correlate with neuronal integrity and mitochondrial function (Ross & Sachdev, 2004). Upregulated mI can reflect combatting osmotic stress to maintain fluid and electrolyte balance (Heikkilä et al., 2009), as well as glial cell activation in response to neuroinflammation (Schneider et al., 2012). Moreover, increases in tCho could be due to structural impairments and inflammation in the brain, as it has been

linked to the cellular phospholipid membrane's damage and repair mechanisms (Ross & Sachdev, 2004).

Other interesting metabolites in the context of T2DM include glutathione (GSH), an antioxidant protecting neurons from oxidative stress (Dwivedi et al., 2020), and glutamate (Glu), the main excitatory neurotransmitter in the brain. Both have been found to correlate with glycemic control. Specifically, d'Almeida et al. (2020) found low Glu in the occipital cortex to be linked to poorly controlled T2DM, defined by high glycated hemoglobin (HbA1c). The existence of glutamatergic changes in diabetes has been observed both in animal models and humans (Hristov et al., 2023) and as a citric acid cycle product, it might offer a proxy for studying the health of energy metabolism (Walls et al., 2015). Likewise, lower levels of anterior cingulate cortex GSH were associated with higher fasting blood glucose and HbA1c in older adults (Hoyos et al., 2022). The relationship could be attributed to oxidative stress, where the antioxidant reserves are overwhelmed by an increase of toxic by-products of mitochondrial metabolism (Dwivedi et al., 2020) over time promoting mitochondrial dysfunction and neurodegeneration (Moreira et al., 2007). Understanding the oxidative stress burden across different brain regions in T2DM might help understand the pathogenesis of diabetic encephalopathy. Additionally, Zheng et al. (2017) studied Glu-Gln cycling and lactate (Lac), an alternative energy substrate in the brain during reduced availability of glucose (Herzog et al., 2013). They found in a mouse model of diabetes that cognitive impairment co-occurs with disruptions in the Glu-Gln- and citric acid cycles, increased anaerobic metabolism, and increased Lac, implicating a neuroenergetic deficit model (Zheng et al., 2016; Zheng et al., 2017). Understanding such interplay of the different neurometabolites could be key to uncovering the biological basis for diabetic encephalopathy.

While high-concentration metabolites can be quantified using standard Point-RESolved Spectroscopy (PRESS), other potentially important metabolites that are present in lower

concentrations or overlap with other signal peaks, like GSH and Lac, would require more specialized protocols and thus have been investigated less (Wu et al., 2017; Zhao et al., 2018). Although the aforementioned study by Hoyos et al. (2022) used PRESS to quantify GSH, the technique may lack precision or underestimate concentrations (Sanaei Nezhad et al., 2017). To overcome such problems, and optimally quantify low-concentration metabolites, the current investigation used a relatively novel MRS sequence that relies on J-difference spectral editing (Oeltzschner et al., 2018) in combination with linear-combination modelling (Oeltzschner et al., 2020).

The primary aim of this study is a full-spectrum exploration comparing default mode network neurometabolism between adults with T2DM and an age-matched non-diabetic control group using $^{1}$H-MRS, contrasting both the main neurometabolites quantified in previous studies (i.e., tNAA, Glx, mI, tCr, tCho) as well as the relatively less-reported metabolites (i.e., GSH, Glu, Gln, Lac). The secondary aim of this study is to explore associations between neurometabolism and peripheral glucose homeostasis. Therefore, this study has two main research questions: (1) what are the neurometabolic differences between adults with T2DM and without T2DM, and (2) are those differences correlated with HbA1c? Identifying potential neuronal markers of metabolic distress will help provide a basis for detailed understanding of T2DM-related cognitive impairment and its mechanisms.



## 2. Methods

### 2.1. Design and Setting.

This was a sub-study of the PROTECTION trial (NCT05023538), conducted at REVAL (Rehabilitation Research Centre) of Hasselt University, the Heart Centre of Jessa Hospital (Hasselt, Belgium) and at the Radiology Department of the University Hospital of Leuven (Leuven, Belgium) between 2022 and 2023. The Central Ethical Committee of the University

Hospital of Leuven approved the study (S65741), and it was conducted in accordance with the Declaration of Helsinki (World Medical, 2001).

**2.2. Participants.**

Adults with T2DM ($n$ = 20) and age- and sex-matched non-diabetic adults ($n$ = 20) were recruited via flyers through local general practitioners, the diabetes support organization Diabetes Liga, and a local public health insurance agency. Additionally, non-diabetic subjects were recruited via social media (Facebook and LinkedIn) and word-of-mouth. Individuals with non-insulin dependent T2DM receiving oral anti-diabetic medication, or untreated with HbA1c ≥ 6.5% were eligible, as well as control subjects with fasting glucose < 126 mg/dl and HbA1c < 6.5%. Because this study was a sub-study of the PROTECTION trial, which involved a longitudinal exercise training intervention, participants were excluded if they were diagnosed with disorders limiting exercise performance, such as chronic heart disease (valve insufficiency ≥ grade 2), sustained ventricular arrhythmias, recent adverse cardiac events (myocardial infarction, coronary artery bypass graft, percutaneous coronary intervention), clinical heart failure, percutaneous coronary intervention, chronic obstructive pulmonary- or renal disease, cerebrovascular or peripheral vascular disease, severe hypertension (> 160/110 mmHg), ongoing cancer, or severe neuropathy. Only a subset of the total participant count of the PROTECTION trial ($N$ = 182) was included in the current study. No additional selection criteria were applied; rather, inclusion was determined by the timing of recruitment (August 2022–May 2023), participants' willingness to undergo an additional MRI scan, and the absence of MRI contraindications.

**2.3. Procedure.**

All participants underwent two hospital visits; (1) fasted blood sampling, and (2) cognitive screening and $^{1}$H-MRS of the brain. The two visits were on average 20 days apart ($SD$ = 11

days). While all participants were fasted for their morning blood sampling appointment, the MRI appointments took place in the evening after normal office hours, post-prandial, to keep the timing as consistent across participants as possible. The exercise training intervention associated with the PROTECTION trial started after both measurement visits had been concluded and thus had no interference with this study.

**2.3.1. Blood Sampling.**

Blood samples were drawn from the antecubital vein in the morning after an overnight fast (≥ 8 h). To obtain plasma and serum fractions, blood tubes were centrifuged for 5 min at 2500 g at room temperature (21°C). The samples were analyzed for lipids, fasting insulin, fasting glucose, and HbA1c. Cobas® kits were used for high-density lipoprotein (HDL) cholesterol (0107528582190c701V5.0), low-density lipoprotein (LDL) cholesterol (0107005768190c701V4.0), insulin (07027559190), and glucose (Alinity kit refG71245R04). Insulin sensitivity was approximated from fasting serum glucose and plasma insulin levels, using the Homeostatic Model Assessment for Insulin Resistance (HOMA-IR; [(Matthews et al., 1985)), calculated as: fasting insulin (mU/l) × fasting glucose (mmol/l) / 22.5. It is known to closely correspond to the gold-standard of hyperinsulinemic-euglycemic clamp measurements (Bonora et al., 2000).

**2.3.2. Montreal Cognitive Assessment (MoCA)**.

The short cognitive screening test comprised several subtests assessing basic cognitive functionality: visuospatial abilities, set shifting, verbal fluency/naming, attention, working memory, delayed recall, abstraction, and orientation. The total score between 0 and 30 reflects overall health of cognitive function. Healthy adults typically score above 26, which is a cut-off score for suspecting mild cognitive impairment (Nasreddine et al., 2005).

**2.3.3. Structural Brain Imaging.**

A 3T Philips Achieva MR scanner (Philips Healthcare, The Netherlands) with a 32-channel receiver head coil was used to obtain a T1-weighted three-dimensional turbo field echo (3DTFE) image (compressed sensing acceleration factor = 2.5, echo time [TE] = 4.6 ms, repetition time [TR] = 9.7 ms, 182 sagittal slices, field-of-view = 242 × 256 × 182 $mm^3$, flip angle = 8°) to ensure accurate voxel placement and tissue correction.

**2.3.4. Proton MRS ($^1$H-MRS).**

Four single-voxel scans were obtained from each participant, with three voxels located in the default mode network (i.e., posterior cingulate cortex [PCC; 30 × 30 × 30 $mm^3$], medial prefrontal cortex [mPFC; 30 × 30 × 25 $mm^3$], left hippocampus [LHIPP; 30 × 15 × 15 $mm^3$]), and a functionally distinct fourth region that our research group has the most prior spectroscopy experience with (Cuypers et al., 2021) – the left primary sensorimotor cortex [LSM1; 30 × 30 × 30 $mm^3$]. The mPFC and PCC voxels were based along the midline of the brain, while the LSM1 and LHIPP were placed in the left hemisphere, the former centralized on the hand motor area, and the latter rotated in sagittal and coronal planes to optimally follow the body of the hippocampus and avoid the inferior horn of the lateral ventricle.

Due to the small volume of the hippocampal voxel, PRESS (transients = 128, TE = 35 ms, TR = 2000 ms) was used, as J-difference-edited MRS scans resulted in insufficient spectral quality. In contrast, for the other voxels, a more complex sequence called HERCULES (Hadamard Editing Resolves Chemicals Using Linear-combination Estimation of Spectra; transients = 320, TE = 80 ms, TR = 2000 ms; (Oeltzschner et al., 2018)) was used. The HERCULES sequence uses multiplexed J-difference editing, applying 20-ms editing pulses in four distinct experiments (Figure 1), allowing to separate metabolites with signal overlap (Oeltzschner et al., 2018). The (A + B + C + D) sum spectrum concentrations were used for all other metabolites, except for GSH and Lac for which the (A - B + C - D) difference spectrum was consulted for the most reliable quantification (Oeltzschner et al., 2018). Interleaved water

referencing was used (transients = 16) to counteract any magnetic field offset that may occur during the symmetrical editing scheme (Edden et al., 2016). For all voxels, the spectral width was 2000 Hz, water suppression was conducted using Multiply Optimized Insensitive Suppression Train (MOIST), and shimming was set to automatic second-order pencil-beam (PB) auto shimming. The minimum reporting standards for in vivo MRS were taken into consideration (Lin et al., 2021). The average spectral quality parameters are reported in the supplementary material.

**2.4. MRS data processing and analysis.**

Osprey version 2.9.2. (Oeltzschner et al., 2020) was used for preprocessing, modelling, and quantification of spectroscopy data. The raw HERCULES spectra were averaged and aligned with the major spectral landmarks, whereas the hippocampal spectra were already automatically averaged by the scanner. Linear combination modelling was used to fit the data to the basis set using a stiff baseline (knot spacing = 0.4 ppm). The full basis sets are listed in the supplementary material.

Osprey uses SPM12 (Statistical Parametric Mapping v7771, Wellcome Trust Centre for Human Neuroimaging, University College, London, UK) to segment the T1-weighted image for conducting a tissue- and relaxation-corrected water scaling using the Gasparovic method (Gasparovic et al., 2006) using the relaxation times (s); $T1_{GM}$ = 1.331, $T2_{GM}$ = 0.110, $T1_{WM}$ = 0.832, $T2_{WM}$ = 0.0792 (Wansapura et al., 1999), and $T1_{CSF}$ = 3.817 (Lu et a., 2005), $T2_{CSF}$ = 0.503 (Piechnik et al., 2009). The derived metabolite concentrations are expressed relative to the unsuppressed water reference and reported in institutional units (i.u.). Voxel tissue fractions were compared and not found to significantly differ between groups (Supplementary Table 2), so any group differences should not be due to systematic differences in voxel composition.

Due to restrictions in reliably resolving NAA and NAAG (N-acetylaspartylglutamate) from each other using 3T $^{1}$H-MRS (Archibald et al., 2025), they were reported together as total NAA (tNAA). Similarly, creatine and phosphocreatine were quantified together as total creatine (tCr), and free choline, glycerophosphocholine and phosphorylcholine as total choline (tCho). All spectra were visually inspected for excessive outer volume effects, baseline contamination, and disruptive spurious echoes (Kreis, 2004). In addition, data points that deviated more than three standard deviations from the group mean, were excluded as outliers.

**2.5. Statistical Analysis.**

JMP® Pro Version 17.0 (SAS Institute Inc., Cary, NC, USA) was used for all statistics. Normality was tested using the Shapiro-Wilk test, so that $p < .05$ was concluded non-normally distributed. Equality of variances was checked with the O'Brien test, and the groups were compared using either a two-tailed independent samples *t*-test (normal distribution, equal variances), a two-sample Wilcoxon signed rank test (non-normal distribution, equal variances), or a Welch's test (normal distribution, unequal variances). An alpha level of 5% was used. Cohen's guidelines (Cohen, 1988) were used for interpreting effect sizes. Lastly, correlation analyses using the Spearman's rho (ρ) were conducted to investigate whether the metabolites covaried with HbA1c. One influential outlier in the T2DM group with HbA1c more than three standard deviations higher than the mean was excluded from these correlations. All statistical comparisons were reported without multiple comparison correction, as this was an explorative study to guide future hypotheses in this research line, making it important to observe all potential patterns in the data.

**3. Results**

The T2DM ($n$ = 20) and control ($n$ = 20) groups were age- and sex-matched, both comprising 15 men and five women ranging between 51 and 73 years old. Fasting glucose, glycated

hemoglobin, and whole-body insulin resistance (HOMA-IR) were significantly higher in the T2DM group (Table 1). In contrast, the groups did not significantly differ in age, BMI, blood cholesterol, blood pressure, or cognitive function. However, MoCA scores ranged (minimum – maximum) between 24 – 30 in the control group, and 13 – 30 in the T2DM group. Five participants in the control group and eight in the T2DM group scored ≤ 26 on MoCA, which could be indicative of mild cognitive impairment (Nasreddine et al., 2005).

Table 1 also lists medication intake. While more of the T2DM subjects are medicated, the control group was also found to use a variety of lipid lowering and antihypertensive medications. Metformin was the most used antidiabetic medication (90% of the sample, $n$ = 18), since insulin-dependent T2DM patients were excluded from the current investigation. Additionally, 20% of the T2DM group were regularly using a sodium-glucose cotrasporter-2 (SGLT2) inhibitor, 15% a glucagon-like peptide 1 (GLP1) agonist, 10% sulfonylurea, and 5% a combined dipeptidyl peptidase-4 (DPP4) inhibitor and metformin product.

During data cleaning, five scans emerged with clearly aberrant spectral line shape, namely substantial baseline contamination caused by outer volume effects or imperfect water suppression rendering metabolite signals clearly distorted (2 x LHIPP [one control, one T2DM], 1 x mPFC [T2DM], and 1 x LSM1 [control]), and one scan with abnormally high frequency drift (-16.72 Hz, $M$ = - 3.71 Hz, $SD$ = 3.14 Hz) leading to a poor model fit and elevated residuals (1 x mPFC [control]). Additionally, two metabolite data points were found to be >3 SDs from the mean and were excluded from the analyses. These were one PCC lactate value (6.08 i.u.) in the T2DM group ($M$ = 1.80, $SD$ = 0.76), and one LHIPP GSH value (5.19 i.u.) in the T2DM group ($M$ = 2.48, $SD$ = 0.60). Excluding them enabled parametric testing of the group differences in PCC Lac and LHIPP GSH.

In Figure 2, the remaining participants' average spectra can be seen displaying good overall data quality. Signal-to-noise ratio and linewidths (listed in the Supplementary Table 1) were found to be within the acceptable range (Wilson et al., 2019). Both the LSM1 and mPFC showed some outer volume lipids between 1.0 and 2.0 ppm, likely due to the voxels' proximity to the skull (Kreis, 2004), but there were no considerable group-differences in the appearance and quality of the spectra. The fluctuations of the creatine frequency throughout the editing sequence have been plotted individually for each scan in the supplementary material (Supplementary Figure 1-6), and suggest good stability for most scans, with a few relatively less stable scans in each region, most noticeable in the control group's mPFC.

Group differences in neurometabolite concentrations were observed (Table 2 and Figure 3). However, all statistical tests were conducted without correction for multiple comparisons, and therefore these findings should be interpreted with appropriate caution. The T2DM group expressed significantly lower prefrontal levels of tNAA ($M_{T2DM}$ = 26.62, *SD* = 3.21) than the control group ($M_{CON}$ = 29.20, *SD* = 2.30), *t*(36) = -2.85, *p* = .007, Cohen's *d* = .92, indicating a large effect size. The same was true for prefrontal tCho ($M_{T2DM}$ = 5.01, *SD* = 0.97; $M_{CON}$ = 5.72, *SD* = 0.71; *t*(36) = -2.56, *p* = .015, Cohen's *d* = .84), posterior cingulate tCr ($M_{T2DM}$ = 20.82, *SD* = 1.64; $M_{CON}$ = 22.00, *SD* = 1.74; *t*(38) = -2.21, *p* = .033, Cohen's *d* = .70, indicating a medium effect size), and hippocampal GSH ($M_{T2DM}$ = 2.48, *SD* = 0.60; $M_{CON}$ = 2.96, *SD* = 0.76; *t*(35) = -2.11, *p* = .042, Cohen's *d* = .70). The rest of the group comparisons were not statistically significant (*p* > .05).

Correlations investigating the relationship between the neurometabolites and HbA1c are visualized in Figure 4. Prefrontal tCho (ρ = -.55, *p* < .001), tNAA (ρ = -.38, *p* = .019), and tCr (ρ = -.39, *p* = .019) showed significant negative correlations to HbA1c. Similarly, PCC tCr was found to have a significant negative correlation to HbA1c (ρ = -.32, *p* = .045). Whereas prefrontal Glu (ρ = .36, *p* = .027), along with left sensorimotor Glu (ρ = .38, *p* = .020), Gln (ρ

= .33, $p$ = .046), mI (ρ = .36, $p$ = .026), and Lac (ρ = .36, $p$ = .026) were positively correlated with HbA1c. The rest of the correlations were not statistically significant.

## 4. Discussion

The aim of this study was to investigate neurometabolic differences between T2DM patients and non-diabetic control subjects. This study was explorative, testing a large number of group comparisons to generate hypotheses for future research, thus forgoing statistical correction for type I error. Firstly, in the group comparison, T2DM was found to be characterized by lower levels of prefrontal tNAA and tCho, lower posterior cingulate tCr, and lower left hippocampal GSH, as compared to the control group. Secondly, the correlation analysis between the metabolites and blood glucose control suggested that higher HbA1c, indicative of long-term-elevated blood sugar, was correlated with lower levels of some metabolites in the mPFC and PCC (tNAA, tCho, tCr), and higher levels of other metabolites in the left SM1 and mPFC (Glu, Gln, mI, Lac).

The relationship between T2DM and prefrontal tNAA is well supported by literature, as a meta-analysis about neurometabolism in T2DM found decreased NAA/Cr in the frontal lobes and the lenticular nucleus (Wu et al., 2017). NAA is a non-essential amino-acid synthesized from aspartate produced in mitochondria by acetyl coenzyme A (acetyl-CoA), a key energetic precursor of the citric acid cycle (Goldstein, 1959). Various neurotoxic signals can reduce the bioavailability of acetyl-CoA and thus the synthesis of NAA (Zyśk et al., 2017), signifying an energetic crisis and reduced neuronal viability. Along the same lines, a recent study demonstrated in an animal model that maintaining normal levels of NAA synthesis is incompatible with mitochondrial dysfunction and adenosine triphosphate (ATP) deficiency in the brain, as acetyl-CoA would be prioritized in the citric acid cycle (Francis et al., 2024).

Smaller prefrontal tCho concentrations were observed in participants with T2DM compared to the control group. The total choline (tCho) signal in $^{1}$H-MRS mostly measures phosphocholine, known to contribute to phospholipid synthesis, and glycerophosphocholine, an osmolyte that is also produced in membrane breakdown (Klein, 2000). Previous research has found a link between T2DM and elevated tCho in frontoparietal and subcortical regions (Wu et al., 2017), typically interpreted as neurodegeneration or inflammation-induced increases in membrane turnover, (de)myelination, or gliosis (Roser et al., 1995; Ross & Sachdev, 2004). Although, there is some evidence that glycerophosphocholine could be upregulated in response to membrane breakdown, and phospholipid precursors like phosphocholine downregulated, which complicates the interpretation of tCho (Nitsch et al., 1992). One study found tCho/Cr increased in the mPFC of glucose intolerant adults compared to healthy control subjects, whereas those with fully developed T2DM displayed reduced levels of tCho/Cr in parietal white matter as compared to both healthy controls and glucose intolerant adults, suggesting some disease-state and region dependence (Sahin et al., 2008). Furthermore, their study observed inverse correlations between HbA1c and frontal cortical NAA/Cr and Cho/Cr, mirroring the findings of the current study. Similarly, a longitudinal rodent study observed decreased hippocampal free choline five weeks after a streptozotocin treatment that triggers the pathogenesis of diabetes (Dong et al., 2019). This is also the timeframe when all the brain energy substrates were at their highest in the streptozotocin treated rats, which might indicate a link between increased energy metabolism and reduced tCho.

Diminished posterior cingulate tCr was also found associated with T2DM. In the brain, creatine maintains energy homeostasis and preserves mitochondrial functioning, due to its ability to store high-energy phosphate for later anaerobic metabolism to ATP and counteract the production of reactive oxygen species (ROS) (Marques & Wyse, 2019). Creatine can also act as an osmolyte (Alfieri et al., 2006) and a neuromodulator, proving to be a versatile

neuroprotective compound (Meftahi et al., 2023). While we cannot distinguish between creatine and phosphocreatine using the current methodology, the decrease in tCr provides tentative support to the idea that this vital neuroprotective energy buffer system might be disrupted or depleted in T2DM. Studies have found depleted creatine kinase in diabetic rats (Maryam et al., 1999), as well as depleted occipital lobe tCr in older adults with the *APOE ε4* allele, a genetic risk factor of AD (Laakso et al., 2003). On the other hand, a systematic review found frontoparietal tCr increasing with age (Haga et al., 2009), and another study found Cr and phosphocreatine upregulated in the hippocampus and striatum of diabetic mice (Choi et al., 2023). One recommendation to gain more clarity would be to use phosphorus MRS ($^{31}$P-MRS), which allows the separate quantification of phosphocreatine and ATP, as well as molecules related to phospholipid membrane dynamics, thus also better elucidating the role of different choline-containing compounds (Santos-Díaz & Noseworthy, 2020).

The observed lower GSH concentrations in T2DM are consistent with previous literature. GSH is a brain-derived antioxidant protecting neurons from oxidative stress caused by ROS as by-products of mitochondrial metabolism (Dwivedi et al., 2020). Chronic hyperglycemia can increase ROS production, disrupting redox balance as the oxidative stress surpasses antioxidative capacity, ultimately promoting mitochondrial dysfunction and neurodegeneration (Moreira et al., 2007). Higher levels of GSH in plasma have been found to preserve cognitive function in a prospective study of older adults without dementia (Charisis et al., 2021), whereas diminished GSH concentrations have been linked to aging, elevated blood glucose, chronic oxidative stress, neurodegeneration (Dwivedi et al., 2020; Hoyos et al., 2022). It must be considered as a limitation of the current study, that unlike in PCC, mPFC and SM1, where GSH was measured using J-difference editing, hippocampal GSH was reported from an unedited PRESS acquisition, which is known to yield less reliable quantifications due to the overlapping resonance peaks (Sanaei Nezhad et al., 2017).

Although observing similar levels of mI, Lac, Glu, and Gln between the groups, we found elevated levels of these metabolites correlated with elevated HbA1c. Previous literature often reports increased mI in T2DM (Wu et al., 2017), and low NAA/mI ratio has been found to be a clinically relevant predictor of cognitive decline (Coutinho et al., 2015). Likewise, glutamatergic changes are a common finding in T2DM research (Hristov et al., 2023; Trivedi et al., 2024). Disruptions in the citric acid cycle, astrocyte-neuron communication facilitating Glu-Gln cycling, and cognitive function have been found linked to elevated Lac in a rodent model of diabetes (Zheng et al., 2016; Zheng et al., 2017). Based on our findings, treating HbA1c as a continuous variable instead of a dichotomous division to diabetes and non-diabetes, may be preferable in future studies to increase sensitivity for subtle neurometabolic alterations.

This investigation was the first to our knowledge to apply the HERCULES sequence to a population with T2DM. This was a strength, as it allowed us to scan the full range of metabolites in four distinct regions of the brain within an hour. It is rare for MRS investigations in this population to include this many regions and metabolites of interest. It allowed us to observe group differences that were specific to the default mode network, rather than globally distributed, which could guide mechanistic studies in preclinical models to specifically target the default mode network of the brain. Another strength is that the spectral quality and voxel tissue composition were very similar across the two groups. Therefore, the neurometabolic differences are unlikely to be caused by systematic differences in acquisition quality or voxel-specific structural differences between the groups. With obesity and dyslipidemia being common comorbidities of T2DM (Iglay et al., 2016), our two groups having equal BMI and cholesterol levels could also be considered a strength of this study, making our group comparison more specific to glycemic differences.

The majority of our T2DM sample used antidiabetic medication, potentially limiting the power of this study, as chronic hyperinsulinemia and insulin resistance have been theorized

to be key drivers of cognitive impairment in T2DM (Chow et al., 2019), and the medication intake may have lowered the T2DM patients' circulatory insulin levels to resemble their non-diabetic peers. Taken together with comparable BMI and cholesterol levels, as well as some impaired fasting glucose values in the control group, this may have hampered our ability to observe group differences in neuroinflammatory markers like mI. The patient sample was cognitively comparable to the control group, hindering the attribution of metabolic findings on neurodegenerative processes only affecting the T2DM group. Nevertheless, the groups are representative of healthy and diabetic adults, as participants with T2DM displayed significantly higher fasted glucose, glycated hemoglobin, and HOMA-IR. Future investigations are urged to find drug-naïve participants to reduce any confounding effects on the neurometabolic profile, screen for neurocognitive function before inclusion, and ensure a more sex-balanced sample to ensure generalizability.

The relatively long echo time (TE = 80 ms) of HERCULES may also have contributed to suboptimal detection of metabolite differences, introducing signal decay caused by T2 relaxation which may confound with the current findings (Landheer et al., 2020; Pell et al., 2012; Simegn et al., 2025). Importantly, the main metabolites showing group differences in this study (i.e., tNAA, tCho, and tCr) have been shown to exhibit low coefficients of variation between short- and long-TE acquisitions, suggesting relative robustness to relaxation-related effects (Hui et al., 2024). Nevertheless, low-concentration metabolites such as GSH might be subject to more uncertainty and should be interpreted with caution. Future edited MRS studies might want to consider implementing a multi-TE sequence such as ISTHMUS (Hui et al., 2024), which may help eliminate the drawbacks of using either short or long TE alone.

Taken together, these findings could be interpreted in the context of a deficit model of brain energy metabolism in diabetic encephalopathy, pointing toward potential disruptions in acetyl-CoA availability, the phosphocreatine-creatine energetic buffer, and redox balance. This

is in line with existing theories postulating that mitochondrial dysfunction is not only characteristic of T2DM (Raza et al., 2015), but also a key mechanism driving diabetes related brain changes (Moreira et al., 2007). The correlations with glycemic control imply an insidious onset rather than a dichotomy between metabolic health and disease. These observations may be instrumental to developing preventative treatments to combat cognitive impairment in T2DM. There is some evidence for oral creatine supplementation increasing the bioavailability of creatine in the brain with promising effects on cognitive function (Forbes et al., 2022; Gualano et al., 2011). Pharmacologically increasing the availability of acetyl-CoA has also been investigated in mouse models of aging, showing promise in preserving mitochondrial function and cognition (Currais et al., 2019). Importantly, increasing physical activity should be considered and evaluated as a cost-effective neurorehabilitation strategy for patients with T2DM, given the well-documented effects on glycemic control, vascular function, and neuronal health (Ashcroft et al., 2024), as well as its potential role in preserving choline concentrations in the aging brain (Matura et al., 2017).



## Statements and Declarations

**Author Contribution Statement. Kia Puustinen:** Conceptualization, Funding acquisition, Project administration, Investigation, Formal analysis, Writing – original draft, Writing – review & editing. **Jitske Vandersmissen:** Investigation, Writing – review & editing. **Tin Gojevic:** Conceptualization, Project administration, Investigation, Writing – original draft, Writing – review & editing. **Georg Oeltzschner:** Methodology, Software, Writing – review & editing. **Helge J. Zöllner:** Methodology, Software, Writing – review & editing. **Kenneth Verboven:** Supervision, Conceptualization, Resources, Writing – review and editing. **Dominique Hansen:** Supervision, Conceptualization, Resources, Writing – review and

editing. **Ilse Dewachter:** Conceptualization, Writing – review & editing. **Melina Hehl:** Methodology, Conceptualization, Writing - review & editing. **Koen Cuypers:** Supervision, Conceptualization, Resources, Writing – review and editing.

**Conflicts of Interests.** G.O. is a paid consultant for Neurona Therapeutics Inc (unrelated to this work). The other authors have no relevant financial or non-financial interests to disclose.

**Funding.** This work was supported by the Research Foundation Flanders grants (G095221N) and (SRN W001325N). KP (1131523N), JV (1129225N), TG (11M2723N), MH (11F6921N) are funded by the Research Foundation Flanders. KP (BOF22INCENT18), JV (BOF24INCENT14), TG (BOF23INCENT01) are additionally supported by the UHasselt Special Research Fund grant. MH is supported by a grant from the KU Leuven (PDMT2/24/077). GO, HJZ, and the development of the Osprey software have been supported by NIH grants (R00AG062230 and R21EB033516).

**Acknowledgements.** Blood samples were processed and stored in collaboration with The University Biobank of Limburg (UBiLim). We also acknowledge and thank master students Emma Smet, Fleur Geurts, Elise Aerts, Laure De Waele, Daver Kahraman, and Stefanie De Prins for their help with participant recruitment and data collection.

**Data availability.** The data that support the findings of this study are available on request from the corresponding author. The data is not publicly available due to privacy or ethical restrictions.

## References

Alfieri, R. R., Bonelli, M. A., Cavazzoni, A., Brigotti, M., Fumarola, C., Sestili, P., Mozzoni, P., De Palma, G., Mutti, A., & Carnicelli, D. (2006). Creatine as a compatible osmolyte in muscle cells exposed to hypertonic stress. *J Physiol*, 576(2), 391–401. https://doi.org/10.1113/jphysiol.2006.115006

Alves, S. S., Silva-Junior, R. M. P. d., Servilha-Menezes, G., Homolak, J., Šalković-Petrišić, M., & Garcia-Cairasco, N. (2021). Insulin resistance as a common link between current Alzheimer's disease hypotheses. *J Alzheimer's Dis*, *82*(1), 71–105. https://doi.org/10.3233/JAD-210234

Archibald, J., Bouchard, A. E., Noeske, R., Shungu, D. C., & Mikkelsen, M. (2025). Test-retest reliability of multi-metabolite edited MRS at 3T using PRESS and sLASER. *bioRxiv* (preprint). https://doi.org/10.1101/2025.06.07.657685

Ashcroft, S. P., Stocks, B., Egan, B., & Zierath, J. R. (2024). Exercise induces tissue-specific adaptations to enhance cardiometabolic health. *Cell Metab*, *36*(2), 278–300. https://doi.org/10.1016/j.cmet.2023.12.008

Bonora, E., Targher, G., Alberiche, M., Bonadonna, R. C., Saggiani, F., Zenere, M. B., Monauni, T., & Muggeo, M. (2000). Homeostasis model assessment closely mirrors the glucose clamp technique in the assessment of insulin sensitivity: studies in subjects with various degrees of glucose tolerance and insulin sensitivity. *Diabetes Care*, *23*(1), 57–63. https://doi.org/10.2337/diacare.28.1.108

Charisis, S., Ntanasi, E., Yannakoulia, M., Anastasiou, C. A., Kosmidis, M. H., Dardiotis, E., Hadjigeorgiou, G., Sakka, P., Veskoukis, A. S., Kouretas, D., & Scarmeas, N. (2021). Plasma GSH levels and Alzheimer's disease. A prospective approach.: Results from

the HELIAD study. *Free Radic Biol Med*, *162*, 274–282. https://doi.org/https://doi.org/10.1016/j.freeradbiomed.2020.10.027

Choi, I. Y., Wang, W. T., Kim, B., Hur, J., Robbins, D. C., Jang, D. G., Savelieff, M. G., Feldman, E. L., & Lee, P. (2023). Non-invasive in vivo measurements of metabolic alterations in the type 2 diabetic brain by (1) H magnetic resonance spectroscopy. *J Neurochem*. https://doi.org/10.1111/jnc.15996

Chow, H. M., Shi, M., Cheng, A., Gao, Y., Chen, G., Song, X., So, R. W. L., Zhang, J., & Herrup, K. (2019). Age-related hyperinsulinemia leads to insulin resistance in neurons and cell-cycle-induced senescence. *Nat Neurosci*, *22*(11), 1806–1819. https://doi.org/10.1038/s41593-019-0505-1

Cohen, J. (1988). *Statistical Power Analysis for the Behavioral Sciences.* https://doi.org/https://doi.org/10.4324/9780203771587

Coutinho, A., Porto, F. H., Zampieri, P. F., Otaduy, M. C., Perroco, T. R., Oliveira, M. O., Nunes, R. F., Pinheiro, T. L., Bottino, C., & Leite, C. C. (2015). Analysis of the posterior cingulate cortex with [18 F] FDG-PET and Naa/mI in mild cognitive impairment and Alzheimer's disease: Correlations and differences between the two methods. *Dement Neuropsychol*, *9*, 385–393. https://doi.org/10.1590/1980-57642015DN94000385

Currais, A., Huang, L., Goldberg, J., Petrascheck, M., Ates, G., Pinto-Duarte, A., Shokhirev, M. N., Schubert, D., & Maher, P. (2019). Elevating acetyl-CoA levels reduces aspects of brain aging. *Elife*, *8*, e47866. https://doi.org/10.7554/eLife.47866

Cuypers, K., Hehl, M., van Aalst, J., Chalavi, S., Mikkelsen, M., Van Laere, K., Dupont, P., Mantini, D., & Swinnen, S. P. (2021). Age-related GABAergic differences in the primary sensorimotor cortex: A multimodal approach combining PET, MRS and TMS. *NeuroImage*, *226*, 117536. https://doi.org/10.1016/j.neuroimage.2020.117536

d'Almeida, O. C., Violante, I. R., Quendera, B., Moreno, C., Gomes, L., & Castelo-Branco, M. (2020). The neurometabolic profiles of GABA and Glutamate as revealed by proton magnetic resonance spectroscopy in type 1 and type 2 diabetes. *PLoS One*, *15*(10), e0240907. https://doi.org/10.1371/journal.pone.0240907

Dong, M., Ren, M., Li, C., Zhang, X., Yang, C., Zhao, L., & Gao, H. (2019). Analysis of metabolic alterations related to pathogenic process of diabetic encephalopathy rats. *Front Cell Neurosci*, *12*, 527. https://doi.org/10.3389/fncel.2018.00527

Duarte, J. (2016). Metabolism in the diabetic brain: neurochemical profiling by 1H magnetic resonance spectroscopy. *J Diabetes Metab Disord*, *3*(011), 10.24966. https://doi.org/10.24966/DMD-201X/100011

Dwivedi, D., Megha, K., Mishra, R., & Mandal, P. K. (2020). Glutathione in brain: overview of its conformations, functions, biochemical characteristics, quantitation and potential therapeutic role in brain disorders. *Neurochem Res*, *45*(7), 1461–1480. https://doi.org/10.1007/s11064-020-03030-1

Edden, R. A., Oeltzschner, G., Harris, A. D., Puts, N. A., Chan, K. L., Boer, V. O., Schär, M., & Barker, P. B. (2016). Prospective frequency correction for macromolecule-suppressed GABA editing at 3T. *J Magn Reson Imaging*, *44*(6), 1474–1482. https://doi.org/10.1002/jmri.25304

Forbes, S. C., Cordingley, D. M., Cornish, S. M., Gualano, B., Roschel, H., Ostojic, S. M., Rawson, E. S., Roy, B. D., Prokopidis, K., & Giannos, P. (2022). Effects of creatine supplementation on brain function and health. *Nutrients*, *14*(5), 921. https://doi.org/10.3390/nu14050921

Francis, J. S., Nguyen, Q., Markov, V., & Leone, P. (2024). Over-expression of N-acetylaspartate synthase exacerbates pathological energetic deficit and accelerates

cognitive decline in the 5xFAD mouse. *J Neurochem*, *168*(2), 69–82. https://doi.org/10.1111/jnc.16044

Gasparovic, C., Song, T., Devier, D., Bockholt, H. J., Caprihan, A., Mullins, P. G., Posse, S., Jung, R. E., & Morrison, L. A. (2006). Use of tissue water as a concentration reference for proton spectroscopic imaging. *Magn Reson Med*, *55*(6), 1219–1226. https://doi.org/10.1002/mrm.20901

Goldstein, F. B. (1959). Biosynthesis of N-acetyl-L-aspartic acid. *Journal of Biological Chemistry*, *234*(10), 2702–2706. https://doi.org/10.1016/S0021-9258(18)69763-7

Gualano, B., Painneli, V. D. S., Roschel, H., Artioli, G. G., Manoel Neves, J., Pinto, A. L. d. S., Da Silva, M. E. R., Cunha, M. R., Otaduy, M. C. G., & Leite, C. D. C. (2011). Creatine in type 2 diabetes: a randomized, double-blind, placebo-controlled trial. *Med Sci Sports Exerc*, *43*(5), 770–778. https://doi.org/10.1249/MSS.0b013e3181fcee7d

Haga, K. K., Khor, Y. P., Farrall, A., & Wardlaw, J. M. (2009). A systematic review of brain metabolite changes, measured with 1H magnetic resonance spectroscopy, in healthy aging. *Neurobiol Aging*, *30*(3), 353–363. https://doi.org/10.1016/j.neurobiolaging.2007.07.005

Hawley, J. A., & Lessard, S. J. (2008). Exercise training-induced improvements in insulin action. *Acta Physiol*, *192*(1), 127–135. https://doi.org/10.1111/j.1748-1716.2007.01783.x

Heikkilä, O., Lundbom, N., Timonen, M., Groop, P.-H., Heikkinen, S., & Mäkimattila, S. (2009). Hyperglycaemia is associated with changes in the regional concentrations of glucose and myo-inositol within the brain. *Diabetologia*, *52*(3), 534–540. https://doi.org/10.1007/s00125-008-1242-2

Heni, M. (2024). The insulin resistant brain: impact on whole-body metabolism and body fat distribution. *Diabetologia*, 1–11. https://doi.org/10.1007/s00125-008-1242-2

Herzog, R. I., Jiang, L., Herman, P., Zhao, C., Sanganahalli, B. G., Mason, G. F., Hyder, F., Rothman, D. L., Sherwin, R. S., & Behar, K. L. (2013). Lactate preserves neuronal metabolism and function following antecedent recurrent hypoglycemia. *J Clin Investig*, *123*(5), 1988–1998. https://doi.org/10.1172/JCI65105

Hoyos, C. M., Colagiuri, S., Turner, A., Ireland, C., Naismith, S. L., & Duffy, S. L. (2022). Brain oxidative stress and cognitive function in older adults with diabetes and pre-diabetes who are at risk for dementia. *Diabetes Res Clin Pract*, *184*, 109178. https://doi.org/10.1016/j.diabres.2021.109178

Hristov, M., Nankova, A., & Andreeva-Gateva, P. (2023). Alterations of the glutamatergic system in diabetes mellitus. *Metab Brain Dis*. *39*, 321–333. https://doi.org/10.1007/s11011-023-01299-z

Hui, S. C., Murali-Manohar, S., Zöllner, H. J., Hupfeld, K. E., Davies-Jenkins, C. W., Gudmundson, A. T., Song, Y., Yedavalli, V., Wisnowski, J. L., & Gagoski, B. (2024). Integrated short-TE and Hadamard-edited multi-sequence (ISTHMUS) for advanced MRS. *J Neurosci Methods*, *409*, 110206. https://doi.org/10.1016/j.jneumeth.2024.110206

Iglay, K., Hannachi, H., Joseph Howie, P., Xu, J., Li, X., Engel, S. S., Moore, L. M., & Rajpathak, S. (2016). Prevalence and co-prevalence of comorbidities among patients with type 2 diabetes mellitus. *Curr Med Res Opin*, *32*(7), 1243–1252. https://doi.org/10.1185/03007995.2016.1168291

Klein, J. (2000). Membrane breakdown in acute and chronic neurodegeneration: focus on choline-containing phospholipids. *J Neural Transm*, 107(8), 1027–1063. https://doi.org/10.1007/s007020070051

Kreis, R. (2004). Issues of spectral quality in clinical 1H-magnetic resonance spectroscopy and a gallery of artifacts. *NMR Biomed*, *17*(6), 361–381. https://doi.org/10.1002/nbm.891

Kullmann, S., Heni, M., Hallschmid, M., Fritsche, A., Preissl, H., & Häring, H. U. (2016). Brain Insulin Resistance at the Crossroads of Metabolic and Cognitive Disorders in Humans. *Physiol Rev*, *96*(4), 1169–1209. https://doi.org/10.1152/physrev.00032.2015

Laakso, M., Hiltunen, Y., Könönen, M., Kivipelto, M., Koivisto, A., Hallikainen, M., & Soininen, H. (2003). Decreased brain creatine levels in elderly apolipoprotein E ε4 carriers. *J Neur Transm*, *110*(3), 267–275. https://doi.org/10.1007/s00702-002-0783-7

Landheer, K., Gajdošík, M., & Juchem, C. (2020). A semi-LASER, single-voxel spectroscopic sequence with a minimal echo time of 20.1 ms in the human brain at 3 T. *NMR Biomed*, 33(9), e4324. https://doi.org/10.1002/nbm.4324

Lin, A., Andronesi, O., Bogner, W., Choi, I. Y., Coello, E., Cudalbu, C., Juchem, C., Kemp, G. J., Kreis, R., & Krššák, M. (2021). Minimum reporting standards for in vivo magnetic resonance spectroscopy (MRSinMRS): experts' consensus recommendations. *NMR Biomed*, *34*(5), e4484. https://doi.org/10.1002/nbm.4484

Lu, H., Nagae-Poetscher, L. M., Golay, X., Lin, D., Pomper, M., & Van Zijl, P. C. (2005). Routine clinical brain MRI sequences for use at 3.0 Tesla. *J Magn Reson Imaging*, *22*(1), 13–22. https://doi.org/10.1002/jmri.20356

Maciejczyk, M., Żebrowska, E., & Chabowski, A. (2019). Insulin resistance and oxidative stress in the brain: what's new? *Int J Mol Sci*, *20*(4), 874. https://doi.org/10.3390/ijms20040874

Marques, E. P., & Wyse, A. T. (2019). Creatine as a neuroprotector: an actor that can play many parts. *Neurotox Res*, *36*, 411–423. https://doi.org/10.1007/s12640-019-00053-7

Maryam, B., Khalil, Z., & Robert, D. H. (1999). Effects of diabetes on creatine kinase activity in streptozotocin-diabetic rats. *Chin Med J*, *112*(11), 1028–1031.

Matthews, D. R., Hosker, J. P., Rudenski, A. S., Naylor, B., Treacher, D. F., & Turner, R. C. (1985). Homeostasis model assessment: insulin resistance and β-cell function from fasting plasma glucose and insulin concentrations in man. *Diabetologia*, *28*, 412–419. https://doi.org/10.1007/BF00280883

Matura, S., Fleckenstein, J., Deichmann, R., Engeroff, T., Füzéki, E., Hattingen, E., Hellweg, R., Lienerth, B., Pilatus, U., & Schwarz, S. (2017). Effects of aerobic exercise on brain metabolism and grey matter volume in older adults: results of the randomised controlled SMART trial. *Transl Psychiatry*, *7*(7), e1172–e1172. https://doi.org/10.1038/tp.2017.135

Meftahi, G. H., Hatef, B., & Pirzad Jahromi, G. (2023). Creatine activity as a neuromodulator in the central nervous system. Arch Razi Inst, 78(4), 1169. https://doi.org/ 10.32592/ARI.2023.78.4.1169

Moreira, P. I., Santos, M. S., Seiça, R., & Oliveira, C. R. (2007). Brain mitochondrial dysfunction as a link between Alzheimer's disease and diabetes. *J Neurol Sci*, *257*(1-2), 206–214. https://doi.org/10.1016/j.jns.2007.01.017

Nasreddine, Z. S., Phillips, N. A., Bédirian, V., Charbonneau, S., Whitehead, V., Collin, I., Cummings, J. L., & Chertkow, H. (2005). The Montreal Cognitive Assessment, MoCA: a brief screening tool for mild cognitive impairment. *J Am Geriatr Soc*, *53*(4), 695–699. https://doi.org/ 10.1111/j.1532-5415.2005.53221.x

Nitsch, R. M., Blusztajn, J. K., Pittas, A. G., Slack, B. E., Growdon, J. H., & Wurtman, R. J. (1992). Evidence for a membrane defect in Alzheimer disease brain. *Proc Natl Acad Sci*, 89(5), 1671–1675. https://doi.org/10.1073/pnas.89.5.1671

Oeltzschner, G., Saleh, M., Rimbault, D., Mikkelsen, M., Chan, K., Puts, N., & Edden, R. (2018). Advanced Hadamard-encoded editing of seven low-concentration brain metabolites: Principles of HERCULES. *NeuroImage*, *185*. https://doi.org/10.1016/j.neuroimage.2018.10.002

Oeltzschner, G., Zöllner, H. J., Hui, S. C. N., Mikkelsen, M., Saleh, M. G., Tapper, S., & Edden, R. A. E. (2020). Osprey: Open-source processing, reconstruction & estimation of magnetic resonance spectroscopy data. *J Neurosci Methods*, *343*, 108827. https://doi.org/10.1016/j.jneumeth.2020.108827

Pell, G. S., Lin, A., Wellard, R. M., Werther, G. A., Cameron, F. J., Finch, S. J., Papoutsis, J., & Northam, E. A. (2012). Age-related loss of brain volume and T2 relaxation time in youth with type 1 diabetes. *Diabetes Care*, 35(3), 513–519. https://doi.org/10.2337/dc11-1290

Piechnik, S. K., Evans, J., Bary, L., Wise, R. G., & Jezzard, P. (2009). Functional changes in CSF volume estimated using measurement of water T2 relaxation. *Magn Reson Med*, *61*(3), 579–586. https://doi.org/10.1002/mrm.21897

Raichle, M. E. (2015). The brain's default mode network. *Annual review of neuroscience*, *38*, 433–447. https://doi.org/10.1146/annurev-neuro-071013-014030

Raza, H., John, A., & Howarth, F. C. (2015). Increased oxidative stress and mitochondrial dysfunction in zucker diabetic rat liver and brain. *Cell Physiol Biochem*, *35*(3), 1241–1251. https://doi.org/10.1159/000373947

Roser, W., Hagberg, G., Mader, I., Brunnschweiler, H., Radue, E. W., Seelig, J., & Kappos, L. (1995). Proton MRS of gadolinium-enhancing MS plaques and metabolic changes in normal-appearing white matter. *Magn Reson Med*, 33(6), 811–817. https://doi.org/10.1002/mrm.1910330611

Ross, A. J., & Sachdev, P. S. (2004). Magnetic resonance spectroscopy in cognitive research. *Brain Res Rev*, *44*(2-3), 83–102. https://doi.org/10.1016/j.brainresrev.2003.11.001

Sahin, I., Alkan, A., Keskin, L., Cikim, A., Karakas, H. M., Firat, A. K., & Sigirci, A. (2008). Evaluation of in vivo cerebral metabolism on proton magnetic resonance spectroscopy in patients with impaired glucose tolerance and type 2 diabetes mellitus. *J Diabetes Complicat*, *22*(4), 254–260. https://doi.org/10.1016/j.jdiacomp.2007.03.007

Sanaei Nezhad, F., Anton, A., Parkes, L. M., Deakin, B., & Williams, S. R. (2017). Quantification of glutathione in the human brain by MR spectroscopy at 3 Tesla: Comparison of PRESS and MEGA-PRESS. *Magn Reson Med*, *78*(4), 1257–1266. https://doi.org/10.1002/mrm.26532

Santos-Díaz, A., & Noseworthy, M. D. (2020). Phosphorus magnetic resonance spectroscopy and imaging (31P-MRS/MRSI) as a window to brain and muscle metabolism: A review of the methods. *Biomed Signal Process Control*, *60*, 101967. https://doi.org/10.1016/j.bspc.2020.101967

Schneider, P., Weber-Fahr, W., Schweinfurth, N., Ho, Y. J., Sartorius, A., Spanagel, R., & Pawlak, C. R. (2012). Central metabolite changes and activation of microglia after peripheral interleukin-2 challenge. *Brain Behav Immun*, *26*(2), 277–283. https://doi.org/10.1016/j.bbi.2011.09.011

Simegn, Gizeaddis L., Song, Y., Murali-Manohar, S., Zöllner, Helge J., Davies-Jenkins, Christopher W., Simicic, D., Hupfeld, Kathleen E., Gudmundson, Aaron T., Muska, E., Carter, E., Hui, Steve C. N., Yedavalli, V., Oeltzschner, G., Dean III, Douglas C., Ceritoglu, C., Ratnanather, J. T., Porges, E., & Edden, R. (2025). A Water Relaxation Atlas for Age- and Region-Specific Metabolite Concentration Correction at 3 T. *NMR Biomed*, *38*(1), e5300. https://doi.org/10.1002/nbm.5300

Sun, H., Saeedi, P., Karuranga, S., Pinkepank, M., Ogurtsova, K., Duncan, B. B., Stein, C., Basit, A., Chan, J. C., & Mbanya, J. C. (2022). IDF Diabetes Atlas: Global, regional and country-level diabetes prevalence estimates for 2021 and projections for 2045. *Diabetes Res Clin Pract*, *183*, 109119. https://doi.org/10.1016/j.diabres.2021.109119

Trivedi, R., Singh, S., Singh, V., Yadav, S., Singh, A. C., Singh, A., Chaurasia, R. N., Kumar, A., & Kumar, D. (2024). Unravelling neuroinflammation-mediated mitochondrial dysfunction in mild cognitive impairment: Insights from targeted metabolomics. *Brain Organoid Systems Neurosci J*, *2*, 64–74. https://doi.org/10.1016/j.bosn.2024.10.001

Walls, A. B., Waagepetersen, H. S., Bak, L. K., Schousboe, A., & Sonnewald, U. (2015). The glutamine–glutamate/GABA cycle: function, regional differences in glutamate and GABA production and effects of interference with GABA metabolism. *Neurochem Res*, *40*(2), 402–409. https://doi.org/10.1007/s11064-014-1473-1

Wansapura, J. P., Holland, S. K., Dunn, R. S., & Ball Jr., W. S. (1999). NMR relaxation times in the human brain at 3.0 tesla. *J Magn Reson Imaging*, *9*(4), 531–538. https://doi.org/10.1002/(SICI)1522-2586(199904)9:4<531::AID-JMRI4>3.0.CO;2-L

Wilson, M., Andronesi, O., Barker, P. B., Bartha, R., Bizzi, A., Bolan, P. J., Brindle, K. M., Choi, I.-Y., Cudalbu, C., Dydak, U., Emir, U. E., Gonzalez, R. G., Gruber, S., Gruetter, R., Gupta, R. K., Heerschap, A., Henning, A., Hetherington, H. P., Huppi, P. S.,…Howe, F. A. (2019). Methodological consensus on clinical proton MRS of the brain: Review and recommendations. *Magn Reson Med*, *82*(2), 527–550. https://doi.org/10.1002/mrm.27742

World Medical, A. (2001). World Medical Association Declaration of Helsinki. Ethical principles for medical research involving human subjects. *Bull World Health Organ*, *79*(4), 373–374.

Wu, G.-y., Zhang, Q., Wu, J.-l., Jing, L., Tan, Y., Qiu, T.-c., & Zhao, J. (2017). Changes in cerebral metabolites in type 2 diabetes mellitus: A meta-analysis of proton magnetic resonance spectroscopy. *J Clin Neurosci*, *45*, 9–13. https://doi.org/10.1016/j.jocn.2017.07.017

Yao, L., Yang, C., Zhang, W., Li, S., Li, Q., Chen, L., Lui, S., Kemp, G. J., Biswal, B. B., & Shah, N. J. (2021). A multimodal meta-analysis of regional structural and functional brain alterations in type 2 diabetes. *Front Neuroendocrinol*, *62*, 100915. https://doi.org/10.1016/j.yfrne.2021.100915

Zhao, X., Han, Q., Gang, X., & Wang, G. (2018). Altered brain metabolites in patients with diabetes mellitus and related complications–evidence from 1H MRS study. *Biosci Reports*, *38*(5). https://doi.org/10.1042/BSR20180660

Zheng, Y., Yang, Y., Dong, B., Zheng, H., Lin, X., Du, Y., Li, X., Zhao, L., & Gao, H. (2016). Metabonomic profiles delineate potential role of glutamate-glutamine cycle in db/db mice with diabetes-associated cognitive decline. *Mol Brain*, *9*(1), 1–9. https://doi.org/10.1186/s13041-016-0223-5

Zheng, H., Zheng, Y., Zhao, L., Chen, M., Bai, G., Hu, Y., Hu, W., Yan, Z., & Gao, H. (2017). Cognitive decline in type 2 diabetic db/db mice may be associated with brain region-specific metabolic disorders. *Biochim Biophys Acta - Mol Basis Dis*, *1863*(1), 266–273. https://doi.org/10.1016/j.bbadis.2016.11.003

Zyśk, M., Bielarczyk, H., Gul-Hinc, S., Dyś, A., Gapys, B., Ronowska, A., Sakowicz-Burkiewicz, M., & Szutowicz, A. (2017). Phenotype-dependent interactions between N-acetyl-L-aspartate and acetyl-CoA in septal SN56 cholinergic cells exposed to an excess of zinc. *J Alzheimer's Dis*, *56*(3), 1145–1158. https://doi.org/10.3233/JAD-160693

**Table 1.**

*Subject Characteristics.*

| | T2DM ($n$ = 20) | | Control ($n$ = 20) | | $t/Z$ | $p$ |
|---|---|---|---|---|---|---|
| | *M* | *SD* | *M* | *SD* | | |
| Age (years) | 62.20 | 4.97 | 61.05 | 5.55 | $t$ = .69 | .494 |
| Weight (kg) | 84.85 | 15.87 | 82.65 | 16.13 | $Z$ = -.49 | .666 |
| BMI (kg/m$^2$) | 28.42 | 4.56 | 27.13 | 4.02 | $t$ = .95 | .347 |
| **Fasted glucose (mg/dL)** | 139.60 | 32.61 | 93.70 | 10.48 | $Z$ = 5.05 | **<.001*** ** |
| Fasted insulin (pmol/L) | 104.50 | 71.38 | 71.32 | 44.50 | $Z$ = -1.48 | .140 |
| **HOMA-IR** | 5.14 | 3.44 | 2.44 | 1.50 | $Z$ = -3.10 | **.002** ** |
| **HbA1c (%)** | 6.66 | 0.66 | 5.44 | 0.25 | $Z$ = 5.34 | **<.001*** ** |
| HDL cholesterol (mg/dL) | 53.05 | 18.62 | 56.20 | 19.34 | $Z$ = -.43 | .665 |
| LDL cholesterol (mg/dL) | 85.15 | 33.58 | 105.75 | 44.89 | $t$ = -1.64 | .109 |
| Systolic BP (mmHg) | 140.68 | 18.47 | 138.30 | 23.25 | $t$ = .36 | .722 |
| Diastolic BP (mmHg) | 84.40 | 9.94 | 85.78 | 11.82 | $t$ = -.40 | .691 |
| MoCA score (0 – 30) | 25.70 | 4.21 | 27.20 | 1.47 | $Z$ = -.71 | .475 |
| Medication intake | | | | | | |
| Metformin (*n*) | 18 | | 0 | | | |
| Other oral antidiabetic (*n*) | 6 | | 0 | | | |
| Lipid-lowering (*n*) | 13 | | 7 | | | |
| β/calcium blockers (*n*) | 8 | | 2 | | | |
| Other antihypertensive (*n*) | 12 | | 1 | | | |
| Antithrombotic (*n*) | 8 | | 0 | | | |
| Psychopharmacological (*n*) | 7 | | 0 | | | |

*Note.* Group means are compared using two-tailed Student's *t* or a two-sample Wilcoxon test (Z) where appropriate. Statistically significant p-values are marked (***** < .05, ****** < .01, ******* < .001). Medication intake is expressed as a count (*n*) expressing the number of participants taking each class of medications in each group. Abbreviations: BMI = body mass index, BP = blood pressure, HbA1c = glycated hemoglobin, HDL = high-density lipoprotein, HOMA-IR = homeostatic model of assessment for insulin resistance, LDL = low-density lipoprotein, *M* = Mean, MoCA = Montreal Cognitive Assessment, *SD* = standard deviation, T2DM = type 2 diabetes mellitus.

**Table 2.**

| | | Choline | Creatine | Glutamate | Glutamine | Glutathione | Lactate | Myo-inositol | N-acetylaspartate |
|---|---|---|---|---|---|---|---|---|---|
| | | *M* (*SD*) | *M* (*SD*) | *M* (*SD*) | *M* (*SD*) | *M* (*SD*) | *M* (*SD*) | *M* (*SD*) | *M* (*SD*) |
| mPFC | CON | 5.72 (0.71) | 22.14 (1.37) | 27.69 (4.88) | 5.26 (2.08) | 6.93 (2.23) | 1.96 (0.34) | 23.26 (2.39) | 29.20 (2.30) |
| | T2DM | 5.01 (0.97) | 21.25 (2.06) | 30.17 (4.71) | 6.03 (1.56) | 6.97 (1.59) | 1.79 (0.93) | 24.08 (3.85) | 26.62 (3.21) |
| | *t(df)* | *t*(36) = -2.56 | *t*(36) = -1.56 | *Z* = 1.55 | *t*(36) = 1.28 | *t*(29) = .06 | *F* = .48 | *F* = .62 | *t*(36) = -2.85 |
| | *p* | **.015*** | .127 | .122 | .208 | .949 | .496 | .436 | **.007**** |
| PCC | CON | 4.08 (0.49) | 22.00 (1.74) | 27.47 (3.34) | 5.56 (1.89) | 7.06 (1.76) | 1.70 (0.76) | 21.34 (1.85) | 29.66 (2.44) |
| | T2DM | 4.11 (0.48) | 20.82 (1.64) | 28.17 (2.26) | 5.50 (1.85) | 6.90 (1.75) | 1.80 (0.76) | 22.62 (2.57) | 29.12 (2.42) |
| | *t(df)* | *t*(38) = .23 | *t*(38) = -2.21 | *t*(38) = .77 | *Z* = -.39 | *t*(32) = -.27 | *t*(33) = .38 | *t*(38) = 1.81 | *t*(38) = -.71 |
| | *p* | .818 | **.033*** | .443 | .695 | .792 | .707 | .079 | .483 |
| LSM1 | CON | 3.98 (0.54) | 17.46 (1.17) | 19.14 (3.20) | 4.24 (1.44) | 4.34 (1.17) | 1.34 (0.49) | 18.47 (1.46) | 29.06 (1.95) |
| | T2DM | 3.88 (0.51) | 17.35 (0.82) | 20.78 (1.86) | 5.06 (1.76) | 4.60 (1.19) | 1.64 (0.61) | 19.57 (2.50) | 29.16 (1.47) |
| | *t(df)* | *t*(37) = -.59 | *t*(37) = -.34 | *F* = 3.77 | *t*(37) = 1.58 | *t*(37) = .69 | *Z* = -1.25 | *F* = 2.85 | *t*(37) = .19 |
| | *p* | .561 | .737 | .062 | .124 | .493 | .211 | .101 | .852 |
| LHIPP | CON | 3.35 (0.37) | 12.36 (1.15) | 26.50 (3.39) † | | 2.96 (0.76) | 0.81 (0.66) | 13.75 (2.11) | 12.46 (1.11) |
| | T2DM | 3.44 (0.46) | 12.01 (1.27) | 26.56 (3.99) † | | 2.48 (0.60) | 1.21 (1.11) | 15.19 (3.01) | 12.60 (1.39) |
| | *t(df)* | | | *t*(36) = .06 | | | | | |
| | *p* | | | .956 | | | | | |

| | | | | | | |
|---|---|---|---|---|---|---|
| *t(df)* | *t*(36) = .70 | *t*(36) = -.89 | *t*(35) = -2.11 | *Z* = .50 | *t*(36) = 1.71 | *Z* = .38 |
| *p* | .486 | .381 | **.042*** | .617 | .097 | .704 |

*Group Comparison of Neurometabolite Concentrations (i.u.).*

*Note.* Means and standard deviations are reported alongside a test-statistic (independent samples t-test [*t*], Welch Anova [*F*], or Wilcoxon two-sample test [*Z*]) and its p-value (* < .05, ** < .01). † = Glx (i.e., glutamine + glutamate) is reported here due to the lack of sufficient separation due to poorer signal-to-noise ratio. Abbreviations: CON = control, df = degrees of freedom, i.u. = institutional units, LHIPP = left hippocampus, LSM1 = left primary sensorimotor cortex, M = mean, mPFC = medial prefrontal cortex, PCC = posterior cingulate cortex, SD = standard deviation, T2DM = type 2 diabetes.

**Figure names and captions**

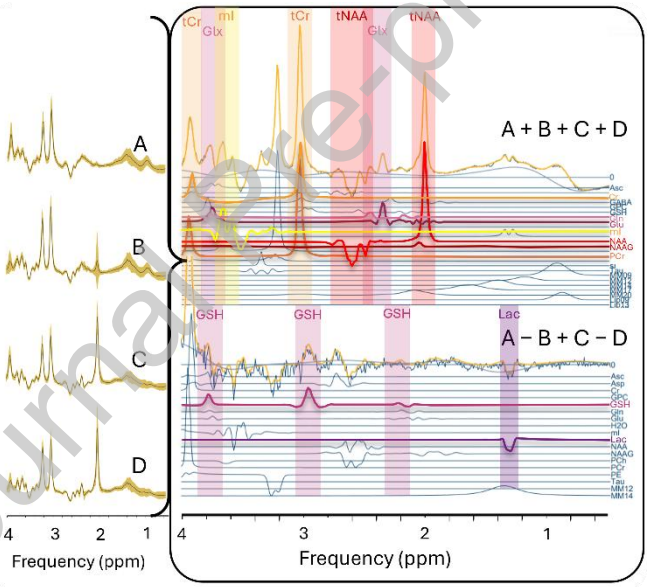


**Figure 1.**

*The Four Distinct Combinations HERCULES Editing Pulses Broken Down to Metabolite Signals.*

*Note.* The HERCULES sequence applies editing pulses at 1.9 ppm to edit GABA, 4.58 ppm to edit GSH, and 4.18 to edit Lac in four different conditions (A, B, C, and D), that are combined into three models (A + B + C + D), (A - B + C - D), (A + B - C + D) for quantifying metabolites.

In this study, the former two of these combination spectra are used to extract all metabolite signals. The figure highlights the origin of each reported metabolite, except for total choline-containing compounds, which is extracted from the sum spectrum (A + B + C + D) as a compound variable of all choline containing signals. Abbreviations: Glx = compound variable of glutamate (Glu) and glutamine (Gln), GSH = glutathione, Lac = lactate, mI = myo-inositol, tCr = total creatine, a compound variable of creatine (Cr) and phosphocreatine (PCr), tNAA = total N-acetylaspartate, a compound variable of N-acetylaspartate (NAA) and N-acetylaspartylglutamate (NAAG).

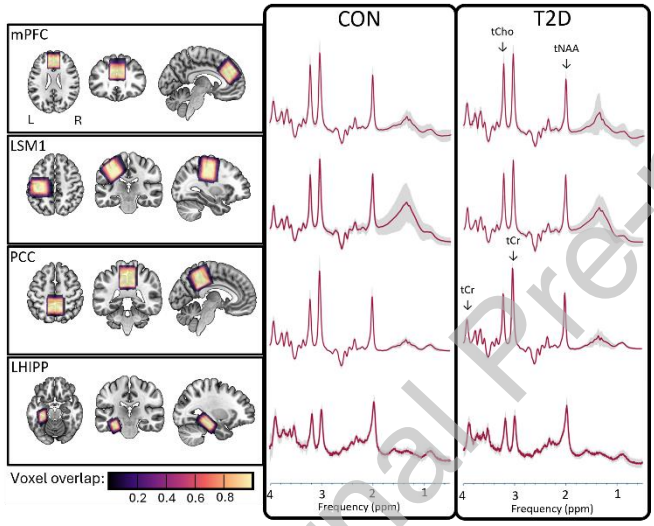


**Figure 2.**

*Voxel Placements and Average Spectra Plotted per Group.*

*Note.* All four $^{1}$H MRS voxel placements are visualized in the SPM152-template standard brain space. Voxel overlap across all 40 participants is visualized in color, showing consistent placement. On the right, the average spectrum per region is plotted for the control group (CON) and type 2 diabetic group (T2DM) along with a grey band marking standard deviation, and arrows indicating significant group differences. Abbreviations: tCho = total choline, tCr = total

creatine, LHIPP = left hippocampus, LSM1 = left primary sensorimotor cortex, mPFC = medial prefrontal cortex, tNAA = total N-acetylaspartate, PCC = posterior cingulate cortex.

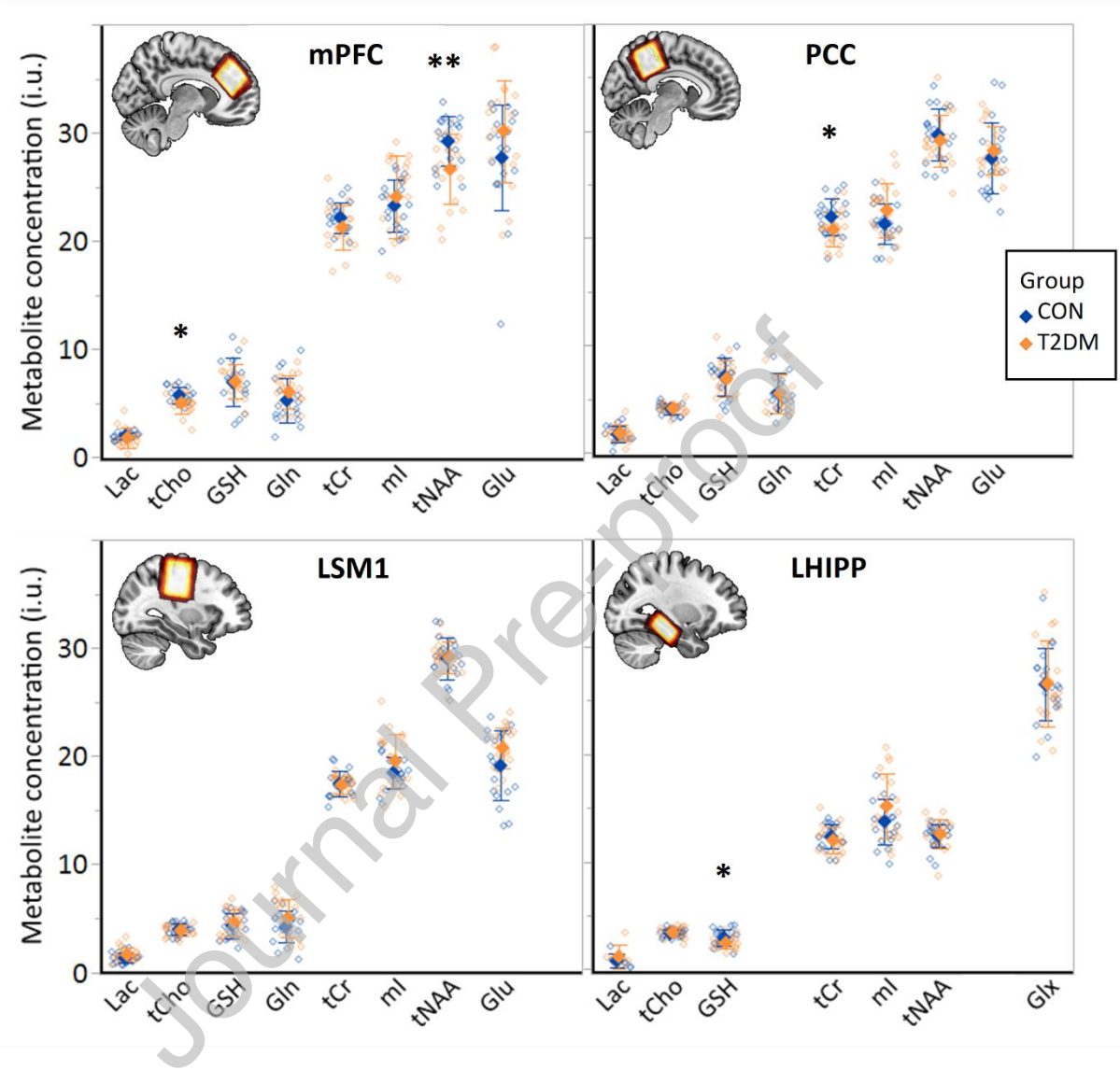




**Figure 3.**

*Neurometabolite Differences in Key Areas of the Default Mode Network.*

*Note.* Mean tissue composition-corrected and water-referenced metabolite levels are compared between patients and control participants. The average concentrations (filled diamonds) and

raw data points (unfilled diamonds) are visualized along with error bars to signify the standard error of the mean. Glx is omitted for the regions where Gln and Glu were quantified separately, and vice versa. Statistically significant t-test p-values are marked: * < .05, **< .01. Abbreviations: tCho = total choline, CON = control group, tCr = total creatine, Glu = glutamate, Gln = glutamine, Glx = glutamine + glutamate, GSH = glutathione, Lac = lactate, LHIPP = left hippocampus, LSM1 = left primary sensorimotor cortex, mI = myo-inositol, mPFC = medial prefrontal cortex, tNAA = total N-acetylaspartate, PCC = posterior cingulate cortex, T2DM = type 2 diabetes mellitus.

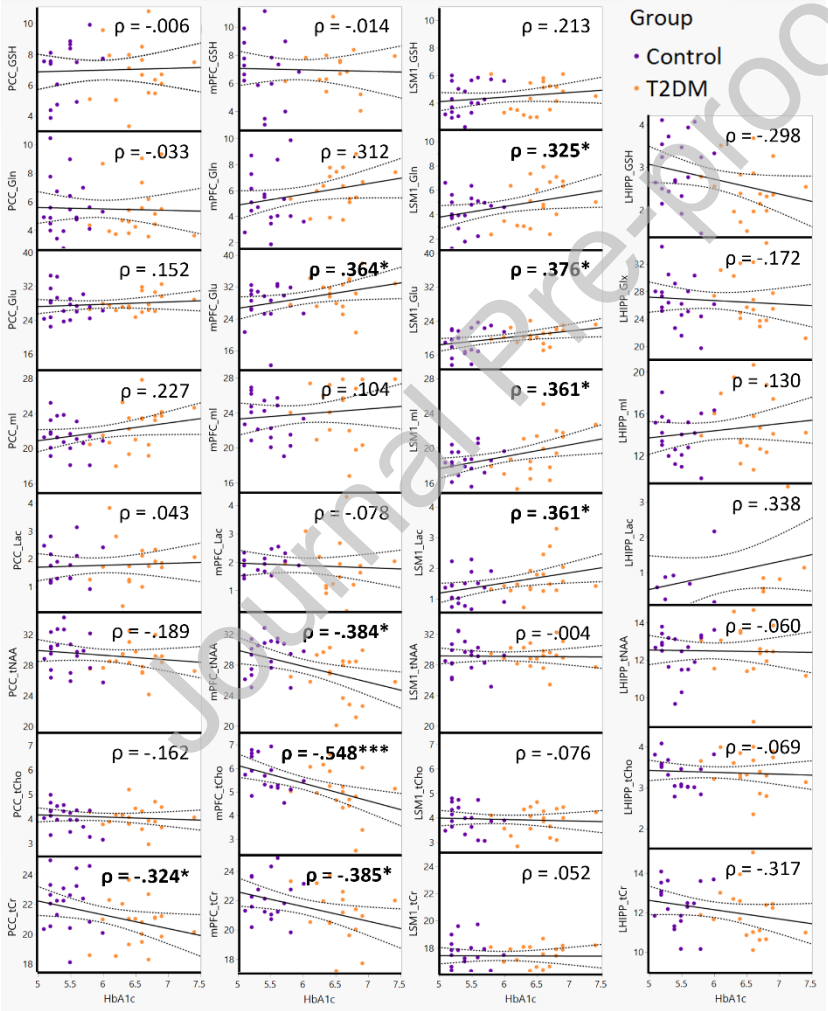


**Figure 4.**

*Scatterplots and Spearman's Correlation Coefficients for Neurometabolites and HbA1c.*

*Note.* Correlation analyses investigating the relationship between the neurometabolites and peripheral glycemic control. Each data point is visualized, and group division is indicated by color (purple = control, orange = T2DM). Statistically significant correlations are marked with asterisks: * < .05, **< .01, ***< .001. Abbreviations: GSH = glutathione, Gln = glutamine, Glu = glutamate, Glx = glutamine + glutamate, Lac = lactate, LHIPP = left hippocampus, mI = myo-inositol, mPFC = medial prefrontal cortex, PCC = posterior cingulate cortex, tCho = total choline, tCr = total creatine, tNAA = total N-acetylaspartate, T2DM = type 2 diabetes mellitus.



## Data Availability Statement

The data that support the findings of this study are available on request from the corresponding author. The data is not publicly available due to privacy or ethical restrictions.

## Graphical abstract

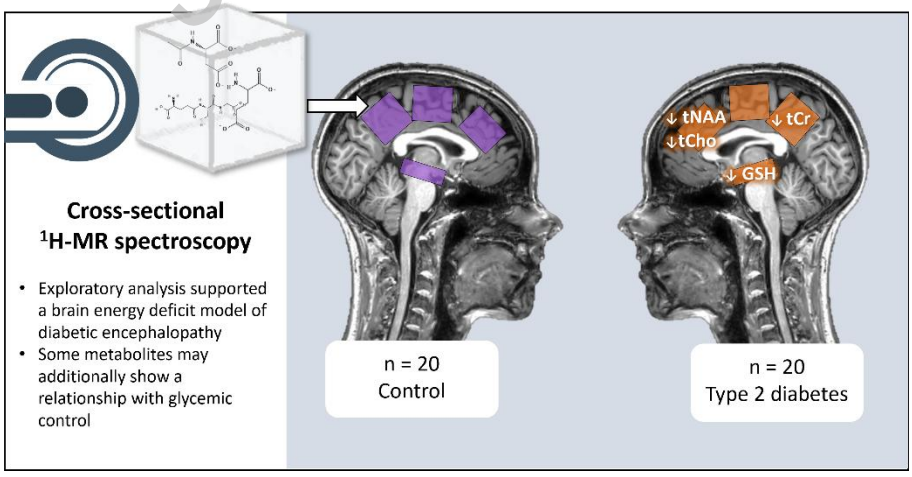

**Declaration of interests**

☐ The authors declare that they have no known competing financial interests or personal relationships that could have appeared to influence the work reported in this paper.

☒ The authors declare the following financial interests/personal relationships which may be considered as potential competing interests:

Georg Oeltzschner reports a relationship with Neurona Therapeutics Inc that includes: consulting or advisory. If there are other authors, they declare that they have no known competing financial interests or personal relationships that could have appeared to influence the work reported in this paper.